ELSEVIER

Journal of Contaminant Hydrology 39 (1999) 91–108

JOURNAL OF
Contaminant
Hydrology

# Retention of liquid contaminants in layered soils

Gabriele S. Walser [a], Tissa H. Illangasekare [b,*], Arthur T. Corey [c]

[a] *TRC Hydro-Geo Consultants, 18925 West 59th Drive, Lakewood, CO 80403 USA*
[b] *Environmental Science and Engineering, Colorado School of Mines, Golden, CO 80401-1887 USA*
[c] *Colorado State University, 1309 Kirkwood Drive, No. 601, Fort Collins, CO 80525 USA*

Received 15 January 1998; received in revised form 10 December 1998; accepted 10 March 1999

**Abstract**

Observations of organic contaminant liquids retained in layered soil profiles indicate contaminant saturations much greater than residual, where residual saturation would be expected, if one assumes a static distribution of fluid pressure. It is theorized that the increased retention of fluid is caused by coarse soil layers that reach a very small unsaturated hydraulic conductivity early in the drainage process, and thus prevent further drainage. The results from a retention experiment in a one-dimensional column were used to test this hypothesis. A vertical column was dry packed with a layer of fine sand (high entry pressure head) overlaying a layer of coarse sand (low entry pressure head). The column was saturated with an organic liquid and then drained. The saturation and pressure profiles were monitored over an extended period of time. A dual-gamma system was used to determine the liquid saturation, and specially fitted ring tensiometers were used to measure the capillary pressure at selected points along the column. The pressure readings and saturation profiles showed a high retention of oil in the fine layer above the interface of the two soils. The profiles were compared first with static pressure and corresponding saturation profiles, and secondly with profiles calculated assuming a very small steady flow through the column. The experimental profiles closely resemble those profiles that assume small flow rates, and display a much higher retention above coarse layers than the static profiles. 

*Keywords:* Vadose zone; Non-aqueous phase liquids; Laboratory experiments; Capillary pressure; Saturation; Dual-energy gamma radiation

## 1. Introduction

Spills of organic chemicals and waste products in the form of non-aqueous phase liquids (NAPLs) have the potential to contaminate groundwater. Accidental spills at the

* Corresponding author. Tel.: +1-303-384-2126; fax: +1-303-273-3413; e-mail: tillanga@mines.edu

0169-7722/99/$ - see front matter 
PII: S0169-7722(99)00029-7

soil surface, or chemicals entering the soil from leaking underground storage tanks, result in the chemical travelling through the unsaturated zone before reaching the groundwater in the saturated zone. Recent research has focused on the infiltration of the NAPL contaminant and its movement with the groundwater, e.g., Illangasekare et al. (1994), Mercer and Cohen (1990). After migration through the vadose zone, a significant fraction of the contaminant is retained in the unsaturated soil. These retained chemicals act as a continuous source of contamination, as small amounts of the fluid continue to move within the soil or partition into aqueous and gaseous phases. A rising water table that results from transient behavior of the regional groundwater system may also mobilize large amounts of the contaminant in the vadose zone. Thus, to design cleanup methodologies, it is necessary to evaluate the process of retention and quantify the entrapment saturations based on the characteristics of the spilt fluids and the soils underlaying the spill. Schwille (1967) performed a number of qualitative experiments of oil infiltration into layered material. He observed that in stratified media, higher oil contents were measured at the boundary between less permeable and more permeable layers. Huntley et al. (1994) investigated the distribution and mobility of a light non-aqueous phase liquid (LNAPL) in the subsurface and related the results to observations of hydrocarbons in monitoring wells. The authors found that the saturation of the LNAPL in most bore holes cannot be described as a smooth function. Variations from the expected smooth saturations correlated qualitatively with variations in soil texture. All bore holes showed higher hydrocarbon saturation above the actual oil saturated zone than predicted by theory. Huntley et al. attributed this observation to non-equilibrium effects which violate the assumption of a hydrostatic pressure distribution invoked by both Farr et al. (1990) and Lenhard and Parker (1990). The authors observed that significant heterogeneities occur on a relatively small scale at their site, which appear to directly impact the hydrocarbon saturation profile. Results similar to these field results have also been shown in our laboratory experiments (Illangasekare et al., 1995).

Cary et al. (1994) conducted infiltration experiments in layered sand columns. The columns contained three layers of soil, with the top layer between 10 cm and the middle layer 6 cm deep. The bottom layer contained the same soil as the top layer, with the middle layer containing a soil of different texture. First, water, and 4 h later, one of three oils (or in reverse order) were added to the columns. After 8 h, the columns were destructively sampled. The results were modeled with an explicit, one-dimensional, multiphase flow code. Of several interesting experimental results, the result of one of their tests is very similar to the results demonstrated in our research. A layer of sand (high entry pressure head of 23 cm) above a layer of loamy sand (low entry pressure head of 3 cm) retained a significant amount of water at the last sampling time (8 h). (The introduction of a second liquid phase did not play any role in this result, since in four cases, the oils had not infiltrated far enough to even reach the coarse layer after 8 h.) The authors conclude that the larger pores of the loamy sand act as a capillary break for the finer sand above it. The numerical code did not model the capillary break and failed to predict this retention of the wetting fluid.

The objective of this research was to develop an experimental program to investigate and obtain accurate data on retention in layered sand in vertical soil columns. We will show that retention occurs where a fine layer overlays a coarse layer. The amount of

retained liquid does not decrease measurably over a significant amount of time. However, a static pressure distribution cannot explain the retention, and a pressure profile assuming steady flow is needed to create saturation profiles closely resembling those found in the experiments.

## 2. Experimental procedures

Experiments were conducted to measure the capillary pressure–saturation curve in order to obtain the parameters describing the coarse and the fine sand. Saturations and pressures were monitored during an extended retention experiment.

### *2.1. Parameter estimation for sand and contaminant liquid*

Two sands, identified by characteristic mesh size as number #30 sand and #125 sand were selected as test material for the experiments. The #30 sand was a coarse, crushed sand, and #125 was a fine natural sand. Soltrol 220, a lighter than water, non-volatile oil, was chosen as the test liquid. Soltrol, and for comparison, water density and viscosity are displayed in Table 1. The oil is the wetting fluid in an oil–air system. The following parameters for both sands were estimated with Soltrol as the wetting fluid for use in the analysis: entry pressure head, Brooks–Corey $\lambda$, residual saturation, maximum natural saturation and saturated hydraulic conductivity (Table 2). Additionally, the properties of both sands and the oil are described in detail in Illangasekare et al. (1994).

The capillary pressure–saturation relation for drainage of Soltrol in #30 sand was measured first in a column packed homogeneously with sand using the gamma system and secondly in a flexible wall permeameter with the flow-pump method (Walser, 1995). The capillary pressure–saturation relation with Soltrol in #125 sand was measured only in the column with the gamma system (described below). From the capillary pressure–saturation data, the entry pressure head, Brooks–Corey $\lambda$ and residual saturation were estimated. Maximum natural saturation with entrapped air was estimated from the gamma measurements of the saturated column for both sands.

Water-saturated hydraulic conductivity for both sands was measured with the flexible wall permeameter flow-pump method (Mapa et al., University of Colorado, unpublished data, 1994). Using the ratio of the viscosities and densities, the water hydraulic conductivity was converted to the Soltrol-saturated hydraulic conductivity.

Table 1
Fluid properties at 23°C

| Fluid | Density, $\rho$ (kg cm$^{-3}$) | Viscosity, $\nu$ (centi Stokes) |
|---|---|---|
| Water | 1000 | 0.94 |
| Soltrol 220 | 789 | 6.12 |

Table 2
Sand parameters measured with Soltrol

| Sand | #30, Crushed sand, coarse | #125, Natural sand, fine |
|---|---|---|
| Residual saturation | 0.08 | 0.01 |
| Maximum natural saturation | 0.8 | 0.85 |
| Brooks and Corey $\lambda$ | 7.4 | 1.6 |
| Entry pressure head (cm) | 10.7 | 15.6 |
| Saturated hydraulic conductivity (cm $s^{-1}$) | 0.022 | 0.0011 |

### *2.2. Experimental procedure for retention experiment*

A plexiglass column of 8.25-cm diameter and 160-cm height was filled with a 52-cm layer of #30 coarse sand overlain by a 50-cm layer of #125 fine sand. To avoid creating heterogeneities within each layer during the filling process, the sand was poured

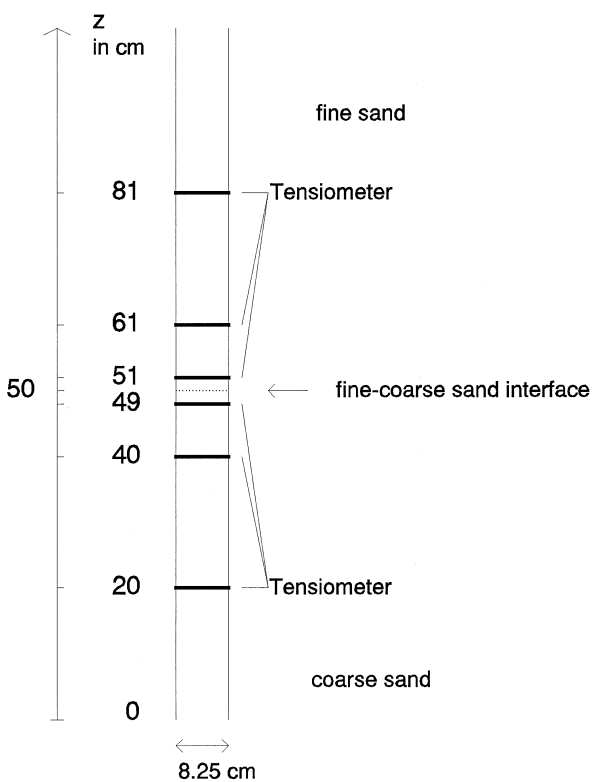


Fig. 1. Schematic of column setup.

into a long tube of smaller diameter, which was placed inside the larger column. The sand was poured into the inner tube and then fell through eight holes (four holes in two sets, located approximately 30 cm and 60 cm above the column end) from the tube into the larger column. By slowly lifting the tube while the sand filled the column, the formation of unintentional sand layers was avoided.

The sand column was then brought to maximum natural saturation with oil (Soltrol 220). Maximum natural saturation was achieved by letting the oil infiltrate slowly over 4 days from the bottom of the column. The sand was then drained to a constant head tank, with the elevation of the oil table in the tank at $z$ equals 0. The oil pressure was monitored continuously with six ring-tensiometers, which were specifically designed and machined for this research. Two of the tensiometers were positioned 1 cm above and below the coarse–fine sand interface, respectively. The remaining tensiometers were 10 and 30 cm above and below the interface. A schematic of the tensiometer locations in the column is shown in Fig. 1. The saturation profile was observed visually, and measured, using the gamma system, along the column in 1-cm intervals. Gamma measurements were conducted 1, 2, 6, 7, 8, 11, 15, and 20 days after drainage in the column had started. Visual inspection of the column continued for 6 months.

*2.2.1. Gamma system*

A dual-gamma attenuation system was used to measure the oil saturation in the column. A radioactive source and a detector for gamma radiation were mounted externally on opposite sides of the sample. Movement of source and detector vertically along the column was automated and this arrangement allowed the measurement of oil saturation at any point along the sample. The oil saturation was calculated from the change in absorption of the gamma radiation between a scan through dry sand and a

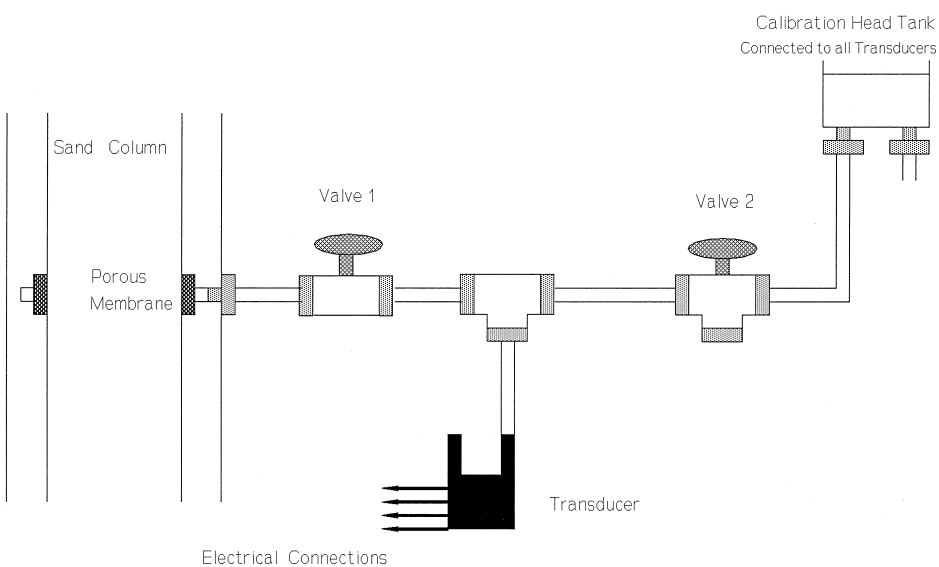


Fig. 2. Column setup with transducers.

scan through the oil wet sand. A detailed description of the gamma system and its accuracy can be found in Illangasekare et al. (1995).

*2.2.2. Tensiometers*

Ring tensiometers similar to those described by Cassell and Klute (1986), and used earlier by Scott and Corey (1961), were used to measure oil pressure in the column. A porous membrane (PORVIC) was glued into a groove cut into the plexiglass tube. The membrane was vacuum saturated with oil, so oil could move freely through the membrane to the transducers (Fig. 2). The transducers were also connected to a calibration head tank, which allowed their calibration at any time during the experiment. A data acquisition system monitored and stored the pressure readings during the experiment.

## 3. Theory

Retention saturation profiles under an assumed static pressure distribution and a small steady state flow are compared to the experimentally determined retention saturations of a contaminant liquid in a layered medium. The derivation of pressure and saturation distribution using both approaches is presented here.

### *3.1. Static retention*

Under static conditions, the piezometric pressure head is constant throughout the system. This necessitates that the capillary pressure head increases linearly with elevation. Hence, for an air–liquid system, it can be written as:

$$p_c = -\rho q z \tag{1}$$

where $\rho$ is the liquid density, $g$ is the gravitational acceleration, $z$ is the height above the zero pressure datum and $p_c$ is the capillary pressure (or capillary suction, since it is negative compared to atmospheric pressure). The saturation in a porous medium is a function of the capillary pressure head (Fig. 3). This functional relationship is called a capillary pressure–saturation relation and can be described with equations by Brooks and Corey (1966).

$$S_e = 1 \quad \text{for } p_c \le p_e \tag{2}$$

$$S_e = \left(\frac{p_e}{p_c}\right)^{\lambda} \quad \text{for } p_c > p_e \tag{3}$$

where $p_e$ is the entry pressure, $S_e$ is the effective saturation, and $\lambda$ is a parameter indicating the pore size distribution. The effective saturation in Eqs. (2) and (3) is defined as:

$$S_e = \frac{S - S_r}{S_m - S_r} \tag{4}$$

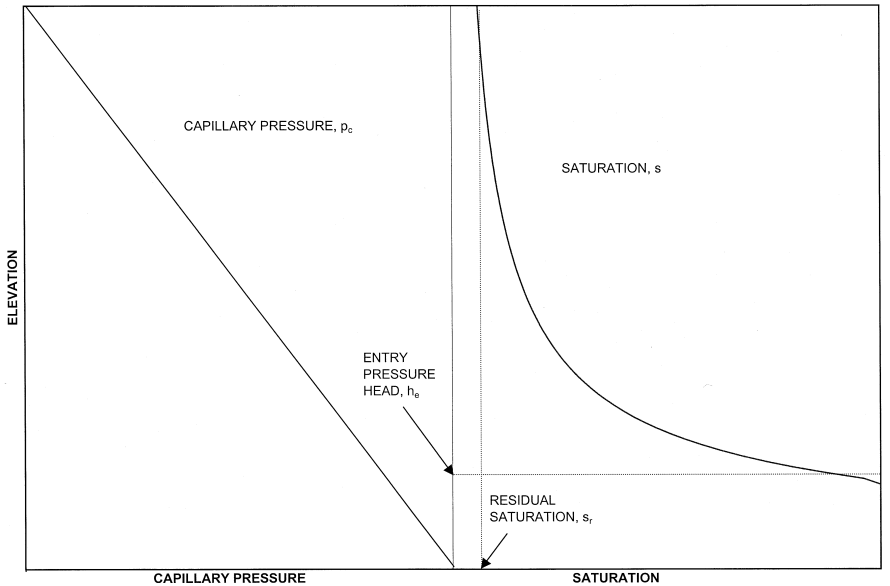


Fig. 3. Characteristic capillary pressure–saturation relation under static pressure distribution.

where $S_r$ is the residual saturation and $S_m$ is the maximum natural saturation with entrapped air ($S_m$ equals 1 for full saturation). The parameters $p_e$, $S_r$, $S_m$, and $\lambda$ are soil characteristics for a given liquid. At true static equilibrium, the distribution of a wetting phase in the unsaturated zone is given by this relation for every layer of a heterogeneous medium. It is assumed that equilibrium has been established by drainage, and that a zero pressure datum exists at an elevation $z$ equals 0. For every soil in the layered system, a unique drainage capillary pressure curve exists. The wetting phase saturation vs. height above a datum can be obtained by combining the capillary pressure curves for each soil on one graph (Fig. 4). Then, one can trace directly the composite representation of $z$ vs. $S$ by noting that the curve for the sand of the lower layer (coarse sand in the example of Fig. 4) is followed over the depth of the lower layer (Collins, 1976). At this point, a discontinuity in saturation occurs, and the pressure–saturation curve for the sand of the upper layer (fine sand in the example of Fig. 4) is followed over the depth of the upper layer.

### *3.2. Retention under steady state flow*

In a layered system, the layer of least permeability has the dominant influence on flow through the system (Collins, 1976). Although steep hydraulic gradients are often present in a layered system, flow through a series of layers of unsaturated soil can be nearly zero when coarse layers with large, empty pores, with characteristically small unsaturated hydraulic conductivities, are encountered. Unless the piezometric pressure head in the fine upper layer rises to a value near atmospheric, flow through the coarse layer will not occur, because the large pores of the coarse sand cannot be fully saturated at the capillary pressures of the upper region. This leads to the retention of liquids above

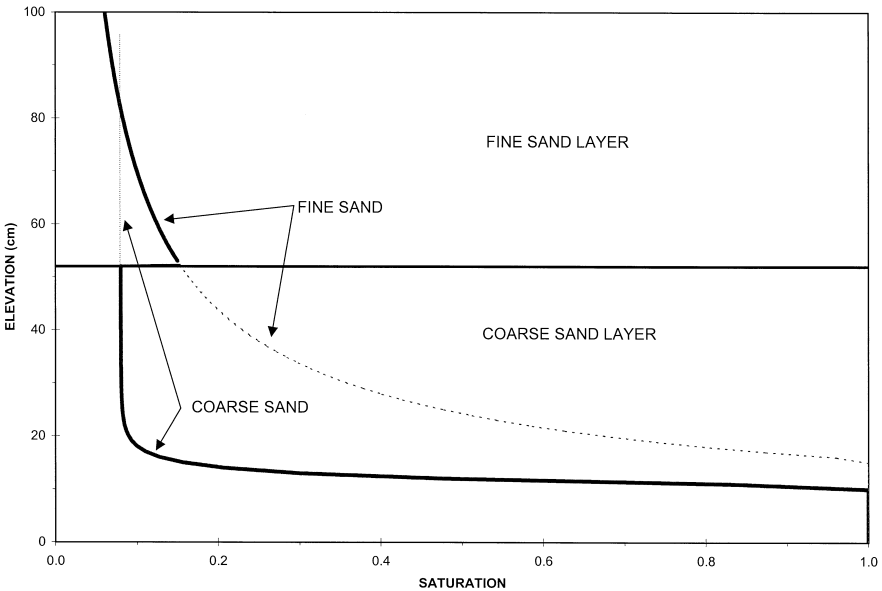


Fig. 4. Static saturation distribution in layered soils.

a coarse layer and a non-static pressure distribution. A static pressure distribution might never be achieved in a layered profile, because the flow may reach a negligible rate in coarse sand.

A steady-state flow model was selected to simulate the pressure and saturation distribution under such low flow rates as may be occurring in layered media. Such a steady-state flow model was first described by Scott and Corey (1961). For downward flow at a steady flux rate, continuity requires that the flux rate be the same in all layers. Also, the liquid is continuous throughout all layers, and thus, the pressure is continuous at all points.

It is assumed that Darcy's law applies to both the wetting (w) and the non-wetting (nw) phase simultaneously. Darcy's law for one-dimensional flow can be written as:

$$q = -\frac{K}{\rho g}\left(\frac{\partial p}{\partial x} + \rho g \frac{\partial z}{\partial x}\right) \tag{5}$$

where $q$ is the Darcy flux, or flow rate per unit cross-sectional area, $K$ is the hydraulic conductivity, $\rho$ is the density of the liquid phase, $g$ is the gravitational acceleration, $p$ is the pressure, $z$ is the elevation head, and $x$ is the coordinate axis.

For one-dimensional unsaturated flow in the vertical direction, $\delta z/\delta x = 1$, and $K$ is the unsaturated hydraulic conductivity. In the case where the non-wetting fluid is air at ambient pressure, $q_{nw} = 0$, $p_{nw} = 0$, and $p_w = -p_c = -h_c \rho_w g$, where $h_c$ is the capillary pressure head. Thereby, Eq. (5) simplifies to:

$$q_w = -K_w\left(-\frac{\delta k_c}{\delta z} + 1\right) \tag{6}$$

where $q_w$ is the Darcy flux in the positive (upward) $z$ direction.

If $q$ is defined as the Darcy flux of the draining wetting fluid in the negative (downward) $z$ direction, Eq. (6) becomes:

$$\frac{\delta k_c}{\delta z} = 1 - \frac{q}{K_w}. \tag{7}$$

$K_w$, the unsaturated hydraulic conductivity, is a function of $h_c$.

$$K_w = f(h_c) \tag{8}$$

The following expression was used to represent $K_w$ (Corey, 1986):

$$K_w = K_m \quad \text{for} \quad h_c \le h_e \tag{9}$$

$$K_w = K_m \left( \frac{h_e}{h_c} \right)^{\eta} \quad \text{for} \quad h_c \ge h_e \tag{10}$$

where $K_m$ is the saturated hydraulic conductivity, $h_e$ is the entry pressure head, and $\eta$ equals $2 + 3\lambda$ (Brooks and Corey, 1966). Combining Eqs. (7) and (10) results in the following integral for $h_c \ge h_e$:

$$\Delta z = \int \frac{1}{1 - \frac{q}{K_m} \left( \frac{h_c}{h_e} \right)^{\eta}} \mathrm{d}h_c. \tag{11}$$

The graphical form of the function under the integral, defined as $f(h_c)$, is shown in Fig. 5. This function exhibits a singularity at the 'critical capillary pressure', i.e., where the denominator of the integral approaches 0. In the numerical integration scheme developed

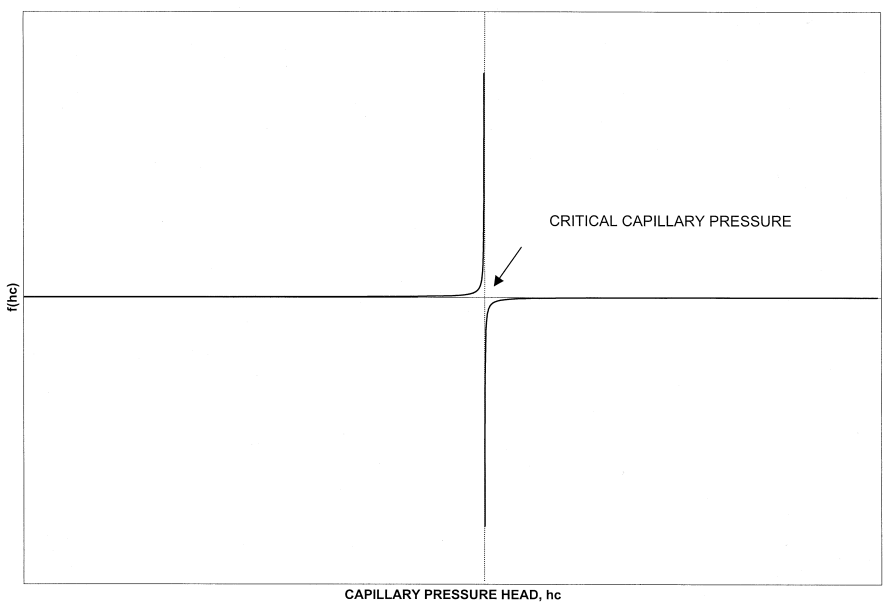


Fig. 5. Critical capillary pressure.

to solve Eq. (11), the pressure approaches the singularity in decreasing steps and at each step verifies that the singularity is not crossed. This process is repeated for every layer. The initial condition for the integration of the first layer is the capillary pressure at elevation $z$ equals 0. With a liquid table at $z$ equals 0, the capillary pressure is equal to 0. The initial condition for every upper layer is the pressure calculated for the top of the layer below it. This condition follows from the requirement that the pressure be continuous throughout the column. Depending on the initial condition, the integration takes place on the left or the right branch of the function shown in Fig. 5.

The resulting pressure distribution shows no discontinuity in capillary pressure. However, abrupt changes in saturation occur at the interfaces between different layers, and consequently, abrupt changes in the unsaturated hydraulic conductivity. The saturation distribution is calculated from the pressure distribution using Eqs. (2) and (3).

## 4. Results

The sand parameters were measured, as described previously, and the results are summarized in Table 2. The results for the retention experiment shown here are based on measurements taken 14 days after drainage was started. Twenty-four hours after drainage was started, the flow of Soltrol was too small to be measured, i.e., the volume in the container collecting the draining oil no longer increased visibly. Also, saturation and pressure profiles appeared to be constant from then on. Thus, the saturation and pressure profiles of 14 days are representative for any profiles taken more than 24 h after start of the drainage process. The saturation profile found experimentally and the static saturation profile calculated from the measured capillary pressure–saturation profile are shown in Fig. 6. The experimental saturation profile shows an effective saturation close to one at elevation $z$ equals 0, and again at the fine–coarse sand interface. In the lower layer of coarse sand, the saturation profile follows closely the saturation profile resulting from a static distribution. However, the static model distribution shows a saturation approaching residual for the fine sand throughout its thickness, and does not show the experimentally found fully saturated zone near the interface. The measured capillary pressure also does not approximate the linear static capillary pressure distribution. The experimental data show a capillary pressure which remains relatively constant with elevation in the coarse sand and increases in the fine sand (Fig. 7). The apparent contradiction (that the saturation profile in the coarse sand, shown in Fig. 6, is close to the static profile, while the pressure profile does not match the static profile) can be explained by noting that the pressures measured in the coarse sand are all in the region approaching residual saturation, where even large increases in capillary pressure will not change the saturation significantly. Thus, the saturation is not sensitive to differences in pressures, and the saturation profile matches the static case as well as the steady state case. The difference between static and steady state case here can only be discerned in the pressure profiles.

Experimental saturation and pressure profiles were compared with profiles from the steady state model with a Darcy flux of $3*10^{-7}$ cm $s^{-1}$ (Figs. 8 and 9). The steady state saturation profile shows a discontinuity in saturation at the fine–coarse sand

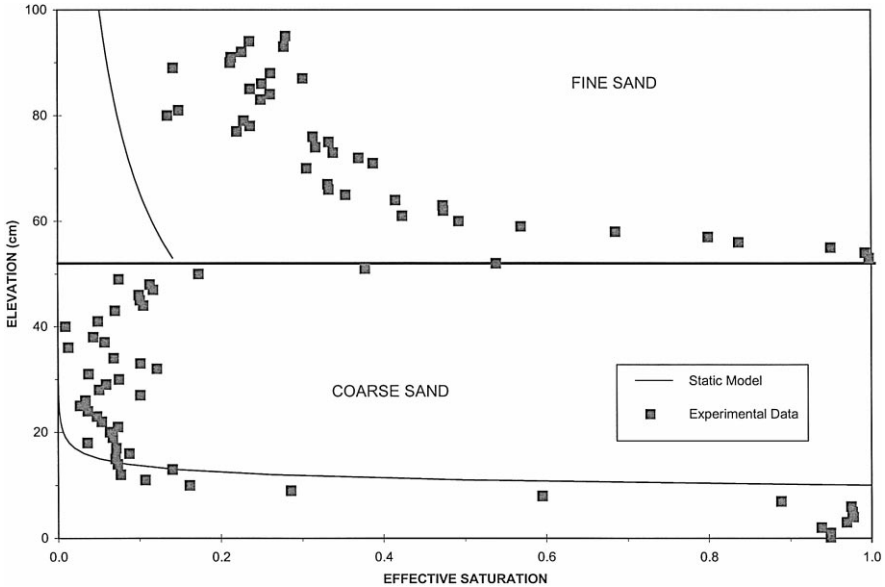


Fig. 6. Experimentally measured saturation profile in layered column in comparison with static model saturation.

interface, which is similar to the experimentally observed jump in saturation. The model saturation profile also approximates the saturation profile in the coarse sand closely. The

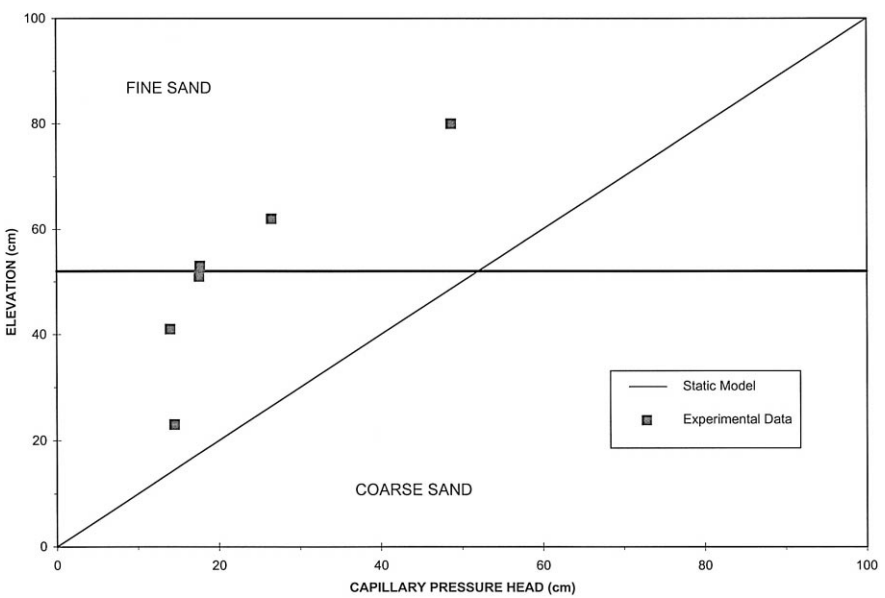


Fig. 7. Experimentally measured capillary pressure head distribution in layered column in comparison with static capillary pressure head distribution.

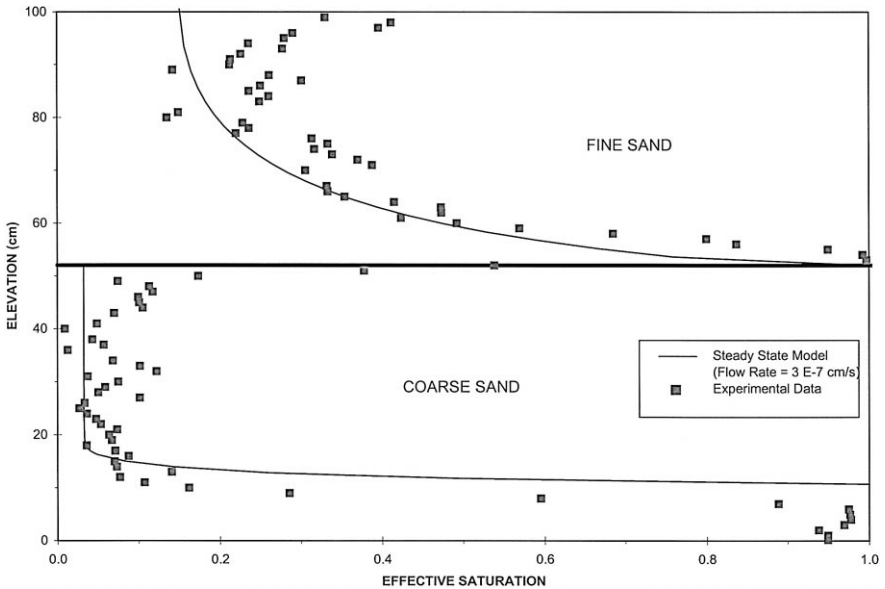


Fig. 8. Experimentally measured saturation profile in layered column in comparison with steady flow saturation profile.

comparison of the pressure profiles shows that the steady state model approximates the measured pressure data well for the assumed flow rate.

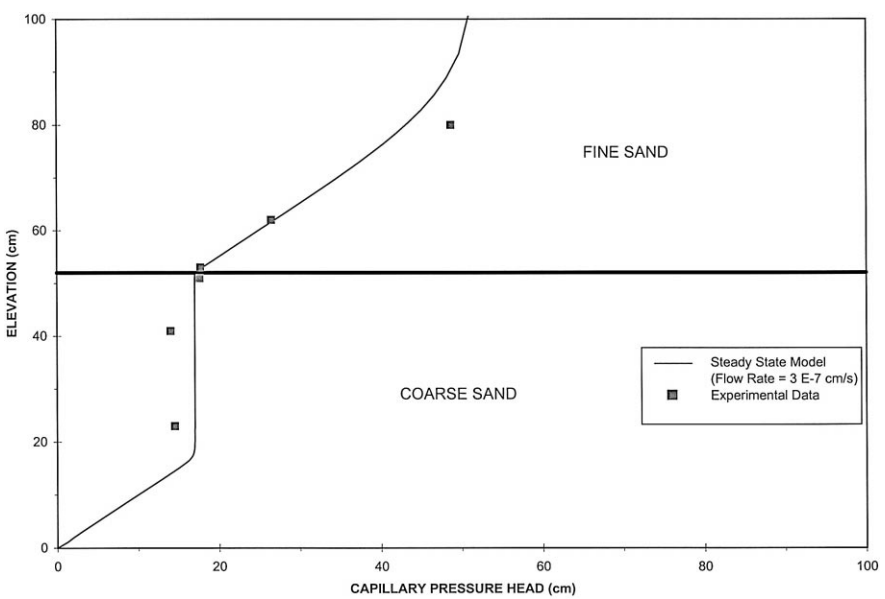


Fig. 9. Experimentally measured capillary pressure head distribution in comparison with steady flow capillary pressure head distribution.

## 5. Discussion

Retention of liquids was observed where a fine layer of sand overlaid a coarse layer. The saturations were found to be stagnant, and no measurable flow was observed through the sand. A comparison with static pressure distribution profiles for capillary pressure head and saturation showed that the experimentally found high saturations at the interface of the layers could be explained under the assumption of a static pressure distribution. Obviously, in spite of having a semi-permanent retention, a static pressure distribution was not achieved. It is believed that the very low hydraulic conductivity of the coarse layer at the boundary (after the coarse layer has de-saturated) caused the flow to be so small that it was not easily observable. Thus, continuing drainage prevented the fluid from achieving a static pressure distribution. Hence, a static pressure distribution did not describe the observed retention even after long periods of drainage.

Assuming that a flow too small to be observed is a more realistic way of modelling the pressure and saturation distribution measured in the column, a model for steady flow was selected to match the observed profiles and to prove that some flow is taking place. A model for steady flow has the advantage of being easily programmed, compared to a fully transient analysis, and is still able to answer the question of whether static conditions or dynamic forces control long-term macro-scale retention. The comparison of the profiles calculated with the steady state model show that the retention profiles match the theoretical profiles very well. A Darcy flux of $3 * 10^{-7}$ cm $s^{-1}$ was found to match the data best. Pressure and saturation profiles for fluxes changed by one order of magnitude from the selected flow are shown in Figs. 10 and 11. The steady state

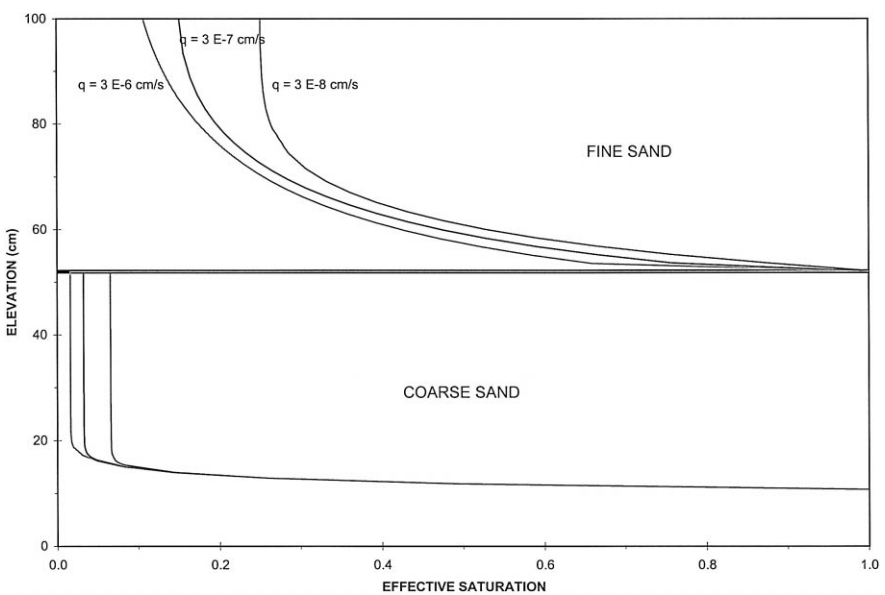


Fig. 10. Sensitivity of saturation profile in layered column to different fluxes.

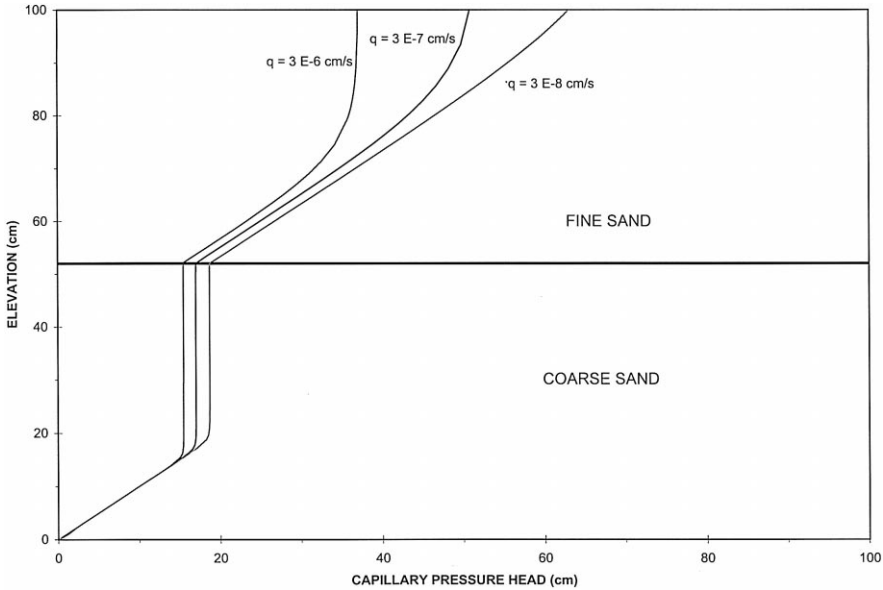


Fig. 11. Sensitivity of capillary pressure head profile in layered column to different fluxes.

solution is not very sensitive to small changes in flow rates, and even order of magnitude changes produce only slightly different profiles. This flow rate was smaller than a flow rate which can be observed using the experimental set-up employed. Thus, it can be concluded that macro-scale retention is controlled by a dynamic process, or more specifically, retention is controlled by the minimum hydraulic conductivity in a soil profile. This minimum hydraulic conductivity exists in the coarse-grained layers, and produces retention where the coarse layer comes into contact with finer-grained layers.

It was observed that the top of the columns had a very low saturation, close to residual; however, the retention zone just above the boundary between the two layers was nearly fully saturated. An assumed steady flow throughout the column results in a saturation profile similar to the one experimentally observed. A steady flow through the upper part of the column is not realistic, since there was no fluid supply at the top of the column. However, a very small flow evidently occurs through the boundary between the fine and coarse material. The head gradient above the boundary is small because of the higher relative conductivity in the nearly saturated region.

The amount of retained liquid does not decrease measurably over a significant time period, because of the extremely small flow rate across the boundary. Thus, it can be proven that the observed pressures (in the layer below the interface and within the more saturated region above the interface) closely approximate pressures found under small steady flows. In reality, the flow rate is transient, but has a very slow rate of change. Thus, it was thought that the assumption of steady flow might provide a useful approximation of the fluid retained above the boundary after prolonged periods of drainage, and clarify the mechanism of dynamic retention.

This finding has consequences when considering remediation of the unsaturated zone. It shows that much higher saturations of a contaminant may be present in layered subsurface systems than one would expect assuming a static pressure distribution. These higher saturations may be modeled by assuming some small steady flow, which can give improved initial conditions for complex numerical models.

## 6. Analysis of the steady state solution

The steady state solution was used to understand the mechanisms controlling retention of contaminant liquids under steady flow. In this section, the properties of the steady state solution are illustrated with example calculations. First, the steady state solution for a homogeneous system is compared to the static solution. Secondly, the steady state solution for a layered system is demonstrated and the dependence of retained liquid on different parameters and variables of the steady state solution is investigated.

Fig. 12 illustrates the difference between a static and a steady flow saturation profile above a zero capillary pressure boundary (equivalent to a water table) in a homogeneous soil. Both profiles were created using the following soil parameters: $K_m$ equals 0.022 cm $s^{-1}$, $h_e$ equals 10.7 cm, and $\lambda$ equals 7.4. Graphed is the effective saturation, which is the saturation normalized with a residual saturation of 0.08. In the static profile, the effective saturation approaches zero above the capillary fringe zone. An effective saturation of zero is equal to residual saturation. The saturation profile resulting from a

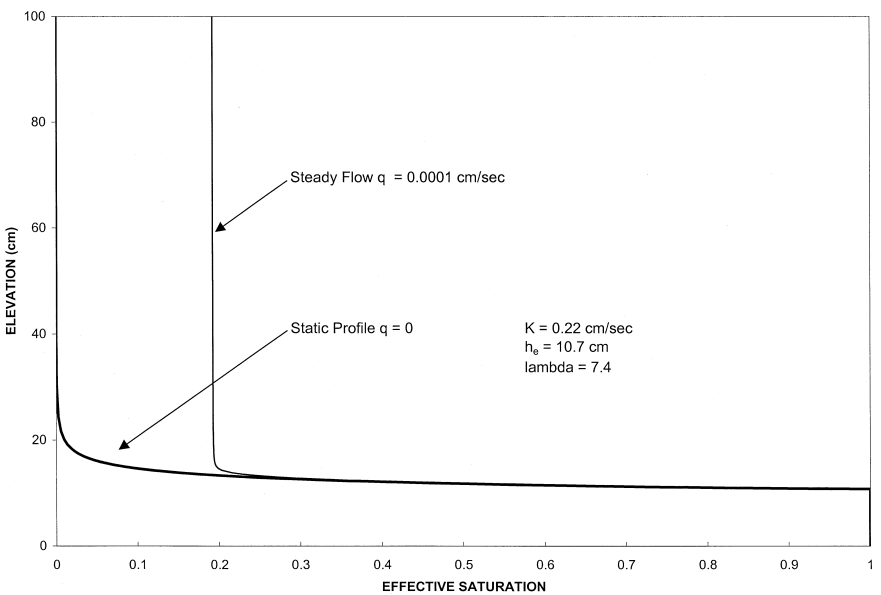


Fig. 12. Saturation profile in a homogeneous soil under static and steady flow conditions.

steady flux of 0.0001 cm $s^{-1}$ approaches an effective saturation of 0.2 above the capillary fringe zone. This saturation correlates to the critical capillary pressure, which is determined by calculating the capillary pressure from the one-dimensional steady state flow solution for the case that the denominator approaches 0:

$$h_{\mathrm{ccrit}} = \left( \frac{K_{\mathrm{m}}}{\mathrm{q}} \right)^{1/\eta} * h_{\mathrm{e}}. \tag{12}$$

The critical capillary pressure head is the pressure under which a certain flux can be maintained with a unit hydraulic gradient for a given sand and fluid. Numerical simulation showed that for these parameters, a flux smaller than $10^{-25}$ cm $s^{-1}$ produces a saturation profile that is essentially equal to the static profile in a homogeneous sand. The higher the flux, the higher is the critical saturation of the steady flow profile.

When the steady flow solution is calculated for a layered system, a constant capillary pressure is reached for every layer, if the layer is thick enough. This is shown in an example in Fig. 13. Both hypothetical sands have equal conductivities and $\lambda$ ($K = 0.022$ cm $s^{-1}$, $\lambda = 7.4$); however, they have different entry pressure heads of 10.7 and 15.6 cm for lower, coarse and upper, fine layers, respectively. The flux used to calculate the profile was $2.2 * 10^{-6}$ cm $s^{-1}$. The critical capillary pressure head is generally higher for finer sands than for coarser sands, as suggested by Eq. (12). However, closer to the interface between two different layers, the critical capillary pressure is not maintained, and the hydraulic gradient is not equal to unity. There is a transition zone in pressure from the critical pressure of one material to the critical pressure of the next material.

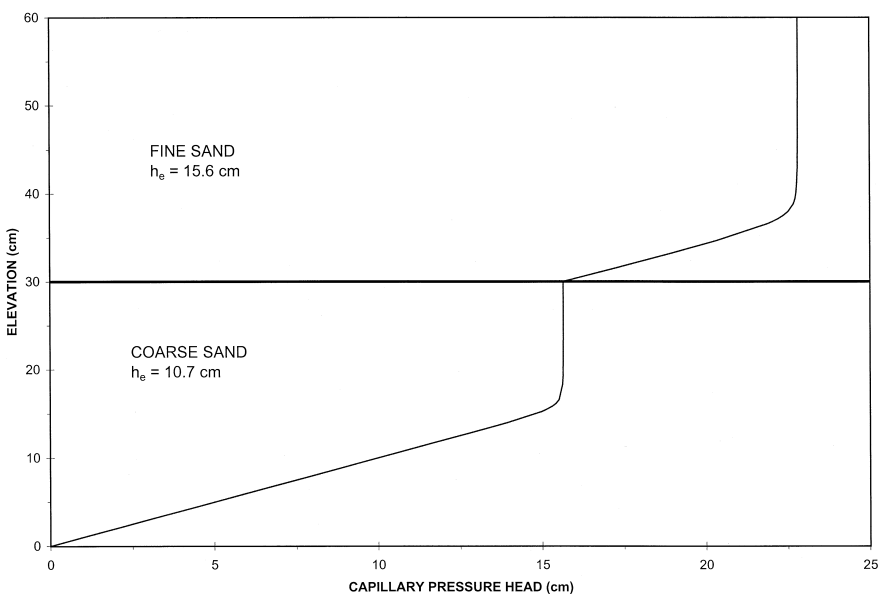


Fig. 13. Capillary pressure in a heterogeneous column with thick layers as computed from the steady state solution.

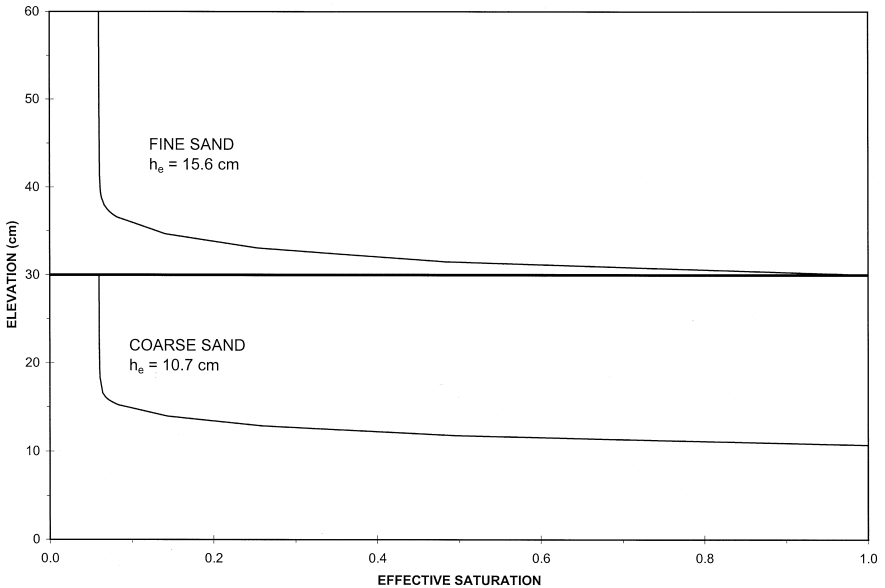


Fig. 14. Saturation profile for a layered soil.

Due to the continuity condition, a jump in pressure cannot occur. If the upper layer has the higher entry pressure (finer soil) the capillary pressure must decrease in the upper layer for downward flow.

The extent of the transition zone determines the amount of retained oil, since the capillary pressure determines the saturation. In Fig. 14, the saturation profile resulting from the capillary pressure profile in Fig. 13 is shown. The increased saturation at the interface is due to the transition in capillary pressure. In this theoretical calculation, the flow rate was adjusted so that the critical capillary pressure of the lower layer was set equal to the entry pressure of the upper layer. Thus, a saturation of unity is only achieved directly at the interface. The extent of the transition zone is controlled by the difference in critical pressure between the two materials. The transition zone is fully saturated as long as the transition capillary pressure is smaller than the entry pressure for the upper layer. As the capillary pressure increases with elevation toward the critical capillary pressure, the saturation decreases toward the values associated with the critical capillary pressure (Fig. 14). Thus, it can be concluded that the amount of oil retained at an interface at a given flow rate is determined by the difference in critical capillary pressure of the lower layer compared to the upper layer. The critical capillary pressure is a function of the soil parameters and the flow rate.

## 7. Conclusions

Macro-scale semi-permanent retention can be observed in layered soil systems. This retention does not follow from a static pressure distribution, but can be modeled better

with a steady state flow assumption. Thus, macro-scale retention is a function of the dynamic soil parameters. The low unsaturated hydraulic conductivities of a coarse sand prevents large flow rates, and with the very small flow rates possible, a semi-permanent retention is observed. This finding has many implications for clean-up strategies, since it shows that contaminant saturations higher than expected when assuming static conditions may be retained in layered soils.

## Acknowledgements

Although this article has been funded in part by the US Environmental Protection Agency under assistance agreement R-819653, through the Great Plains-Rocky Mountain Hazardous Substance Research Center, headquartered at Kansas State University, it has not been subjected to the agency's peer and administrative review and therefore, may not necessarily reflect the views of the agency, and no official endorsement should be inferred.

## References

Brooks, R.H., Corey, A.T., 1966. Properties of porous media affecting flow. ASCE J. Irrig. Drain. Div. 4855 (92), 61–68.

Cary, J.W., Simmons, C.S., McBride, J.F., 1994. Infiltration and redistribution of organic liquids in layered porous media. Soil Science Society of America Journal 58, 704–711.

Cassell, D.K., Klute, A., 1986. Water potential: tensiometry. In: Klute, A. (Ed.), Methods of Soil Analysis: Part 1. Physical and Mineralogical Methods, p. 587.

Collins, R.E., 1976. Flow of Fluids through Porous Materials. Petroleum Publishing, Tulsa, OK, 270 pp.

Corey, A.T., 1986. Mechanics of Immiscible Fluids in Porous Media. Water Resources Publication, Littleton, CO, 255 pp.

Farr, A.M., Houghtalen, R.J., McWorther, D.B., 1990. Volume estimation of light nonaqueous phase liquids in porous media. Ground Water 28, 48–56.

Huntley, D., Hawk, R.N., Corley, H.P., 1994. Nonaqueous phase hydrocarbon in a fine-grained sandstone: 1. Comparison between measured and predicted saturations and mobility. Ground Water 32, 626–634.

Illangasekare, T.H., Znidarcić, D., Walser, G.S., Weaver, J.W., 1994. An experimental evaluation of two sharp front models for vadose zone non-aqueous phase liquid transport. Rep. EPA/600/R/-94/197, U.S. EPA, Ada, OK, 185 pp.

Illangasekare, T.H., Yates, D.N., Armbruster, E.J., 1995. Effect of heterogeneity on transport and entrapment of nonaqueous phase waste products in aquifers: an experimental study. ASCE J. Environ. Eng. 121 (8), 572–579.

Lenhard, R.J., Parker, J.C., 1990. Estimation of free hydrocarbon volume from fluid levels in monitoring wells. Ground Water 28, 57–67.

Mercer, J.W., Cohen, R.M., 1990. A review of immiscible fluids in the subsurface: properties, models, characterization and remediation. J. Contam. Hydrol. 6, 107–163.

Schwille, F., 1967. Petroleum contamination of the subsoil—a hydrological problem. In: Hepple, P. (Ed.), The Joint Problems of the Oil and Water Industries. The Institute of Petroleum, London, England.

Scott, V.H., Corey, A.T., 1967. Pressure distribution during steady flow in unsaturated sands. Soil Science Society Proceedings, pp. 270–274.

Walser, G.S., 1995. Vadose zone infiltration, mobilization and retention of non-aqueous phase liquids. PhD Thesis, University of Colorado, Boulder, April, 255 pp.